2A3-1

Analyses of UWB Spherical Monopole Antenna by Simulation

#Toshitatsu Suzuki [1], Kazuhiro Shibata [2], Somboon Theerawisitpong [1], Yasuo Watanabe [1]
[1] Department of Electrical and Electronics Engineering, Nippon Institute of Technology
4-1 Gakuendai, Miyashiro-machi, Minamisaitama-gun, Saitama-ken, 345-8501, Japan
Tel: +81-480-34-4111, Fax: +81-33-7680
t_szki@m.ieice.org, somboon@wata-lab.com, watanabe@nit.ac.jp
[2] Shinko Industries Inc.
3-28-12 Daita, Setagaya-ku, Tokyo, 155-0033, Japan
Tel: +81-3-3413-9645, Fax: +81-3-3413-9610
s-k-shinkou1974@hkg.odn.ne.jp

1. Introduction

Since the Federal Communications Commission (FCC) released the first report and order of the commission's rules regarding ultra-wideband (UWB) transmission systems in April 2002 [1], the studies on UWB antennas for high-speed communication and high-resolution sensing have been flourishing. One of these UWB antennas is a spherical antenna, whose radiated field in time elapse is investigated in this paper. UWB antennas have historical roots in broadband antenna [2]. Stohr obtained the patent of dipole and monopole antennas using spherical or ellipsoidal radiator, with matching methods of coordinating the distance between half dipoles or the monopole and the reflector or through taper in 1968 [3]. Kraus developed volcano smoke antenna [4][5]. One of the current authors Shibata obtained the patent of spherical monopole antenna on a skewer [6][7]. Recently, Taniguchi and Kobayashi developed a teardrop antenna defined by a finite cone and a sphere [8]. For these spherical shape antennas, there has been few analysis from the point of the radiation field to explain the broadband mechanism.

This paper reports the characteristics derived by simulation on a spherical monopole antenna that consists of a spherical radiator, reflector and coaxial line. The main result is that the sequential behaviour of the electric field and the surface current on the antenna and reflector explicitly show the nature of the travelling wave antenna. The characteristics such as the return loss and the radiation pattern are also presented.

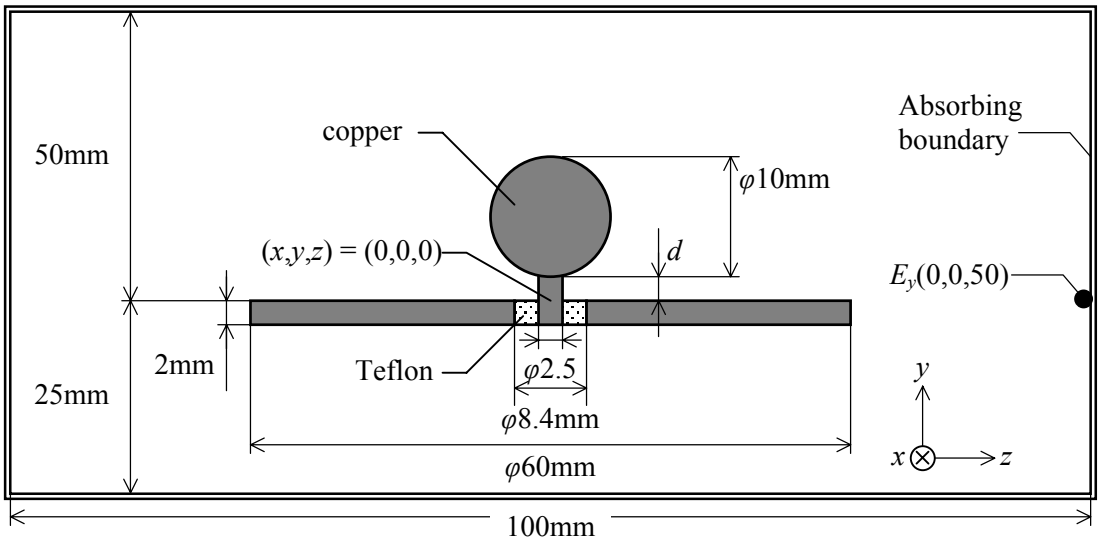

Figure 1: Cross Section of Simulation Model.

ISBN: 978-4-88552-223-9 C3055©IEICE

2. Simulation Model

The simulation model of spherical monopole antenna is shown in Fig. 1. Simulation has been conducted with Micro-stripes 7 of the product by Flometrics, whose algorithm is based on Transmission Line Modelling (TLM) method [9]. The feed line to the sphere is a 50Ω coaxial cable, connected through the centre of the reflector. The discrete size of the space is less than 1mm in order for the frequency range up to 30GHz. For the sphere, the discrete size is especially set to be 0.25mm in order to reconstruct the curved surface in detail.

Stohr mentioned "It is advisable to make the spacing d for the radius r_0 (r_0=one half of the inner diameter of the outer conductor) about equal to r_0, it being assumed thereby that the dielectric has in both ranges the same dielectric constant, above all air." In this paper, with Teflon-filled coaxial cable, d is varied with 0.1mm step to find the optimum value, at which the bandwidth having the return loss being less than –10dB becomes the maximum. The return loss is measured on the coaxial line at the location 0.05mm below the surface of the reflector. Under this optimum condition, the antenna characteristics has been analysed.

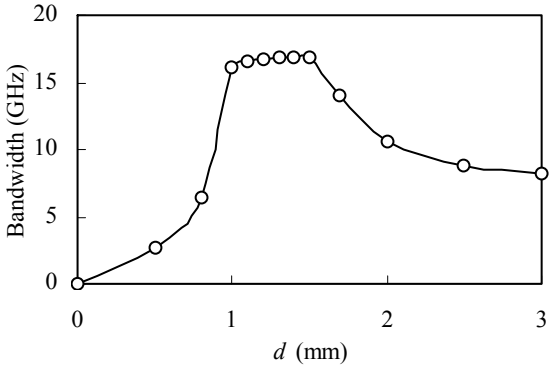

Figure 2: Bandwidth-d Characteristics

3. Simulation Results

First step of simulation is the optimisation of d. Fig. 2 shows the bandwidth with –10dB return loss for various d from 0 to 3mm, and the maximum is obtained at d=1.4. Fig. 3 shows the return loss at d=0 and 1.4mm. For the latter case, the bandwidth is 5.1-22.0GHz and clearly improved than the case at d=0.

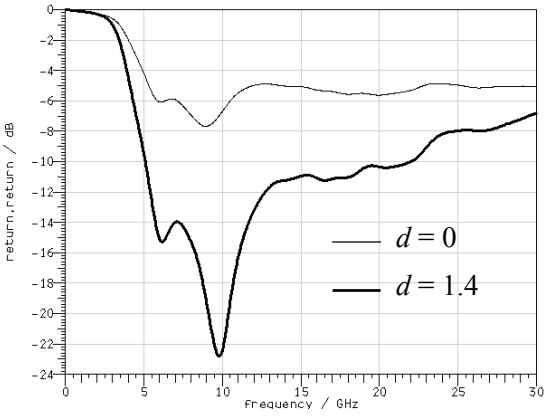

Figure 3: Return Loss

Next, under the optimum value at d=1.4, the antenna characteristics is analysed. As shown in Fig. 4, the feed impedance varies over 25-60Ω relatively in smooth. In Fig. 5 the radiation characteristics in E-plane at 6, 9, 12 and 18GHz are shown and they change gradually. For H-plane, the radiation is omni-directional. Over the full band of 5.1-22.0GHz, the radiation characteristics changes gradually while for a part of the band. In Fig. 6, the amplitude and the phase of the electric field on the horizontal plane and at the radial distance of 50mm from the centre of the reflector are shown. The phase changes almost linearly, indicating only small group delay. The variation of the amplitude is not so smooth due to the dependency of the return loss and the directivity on the frequency. Finally, in Fig. 7 the surface current of the antenna and the electric field distribution in term of the

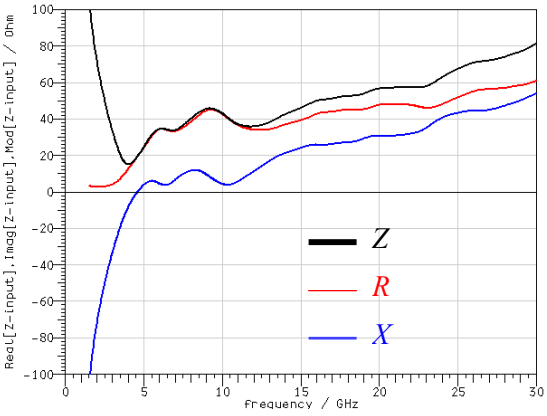

Figure 4: Impedance

absolute value for the frequency of 9.8, 21 and 30GHz are shown in the time elapse expressed as $2\pi ft$ = 0-150deg at every 30deg. In Fig. 7, the surface current propagates unidirectionally from the feeding point to the top of the sphere, and in coupling with it the electric field is radiated. As the travelling wave is predominant, the antenna seems to behave as a travelling wave antenna. The reason for this effect might be caused by the charge distribution that concentrates at the closest region to the reflector, namely at the feed point, and decreases as departing away to the zenith of the sphere, so as the current density follows.

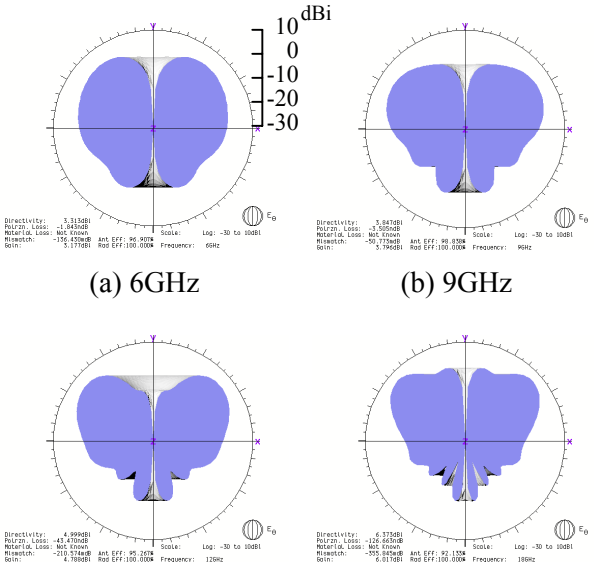

(a) 6GHz (b) 9GHz

(c) 12GHz (d) 18GHz

Figure 5: Radiation Pattern

4. Conclusion

The simulation of TLM method curried on a spherical monopole antenna has visibly shown the movement of the surface current and the radiation field in time elapse, and indicates that the ultra-wideband characteristics of spherical monopole antenna originate in the nature as a travelling wave antenna. The result implies that the other type of UWB antennas might have similar travelling wave behaviours.

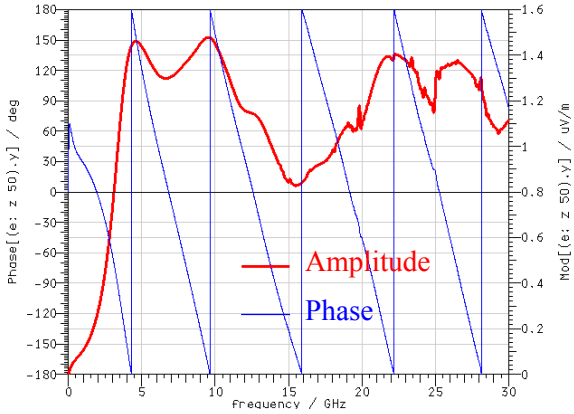

Figure 6: Electric Field

References

[1] Federal Communications Commission, "Revision of part 15 of the commission's rules regarding ultra-wideband transmission systems," First report and order, ET Docket 98-153, FCC 02-48, Adopted: Feb. 14, 2002, Released: April 22, 2002.

[2] H. G. Schantz, "A brief history of UWB antennas," IEEE Aerospace and Electronic Systems Magazine, vol. 19, no. 4, pp. 22-26, April 2004.

[3] W. Stohr, "Broadband ellipsoidal dipole antenna," U.S. Patent 3,364,491, Jan. 16, 1968.

[4] J. D. Kraus and D. A. Fleisch, Electromagnetics with Applications, 5th edition, McGraw-Hill, pp.294-295, 1999.

[5] Lee Paulsen, J. B. West, W. F. Perger and J. Kraus, "Recent Investigations on the Volcano Smoke Antenna," IEEE APS Int. Symp. Vol.3, 845-848, Jun 2003.

[6] K. Shibata, "Antenna," JP Patent 3831141, Oct. 11, 2006.

[7] K. Shibata, "Antenna and its manufacturing method," JP Patent 3785608, June 14, 2006.

[8] T. Taniguchi and T. Kobayashi, "An omnidirectional and low-VSWR antenna for the FCC-approved UWB frequency band," in 2003 IEEE AP-S International Symp., vol.3, pp.460-463, June 22-27, 2003.

[9] C. Christopoulos, The transmission-line modeling method: TLM, IEEE Press, New York, 1995.

[10] C. A. Balanis, Antenna *Theory*, ch. 10, John Wiley & Sons, 2005.

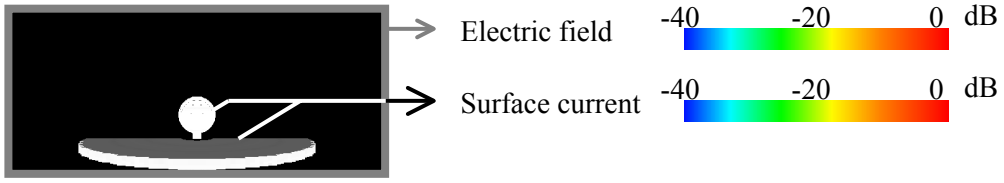

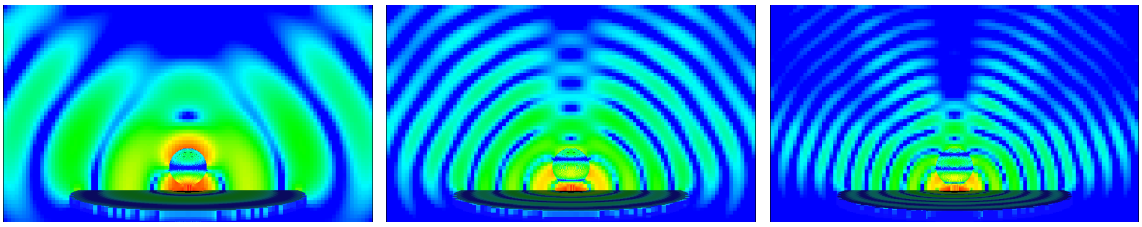

(a) 9.8GHz, 0deg (g) 21GHz, 0deg (m) 30GHz, 0deg

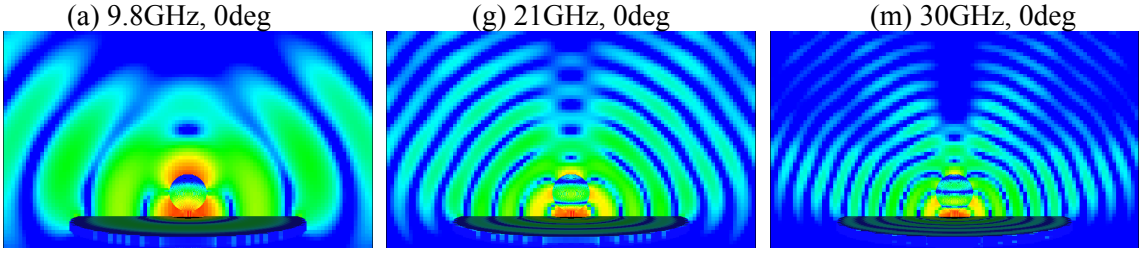

(a) 9.8GHz, 30deg (g) 21GHz, 30deg (m) 30GHz, 30deg

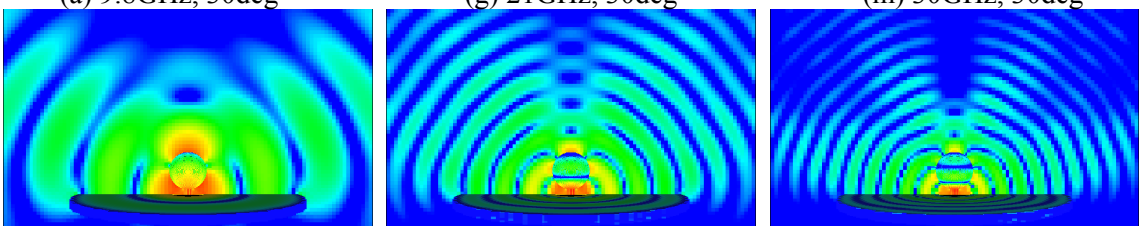

(a) 9.8GHz, 60deg (g) 21GHz, 60deg (m) 30GHz, 60deg

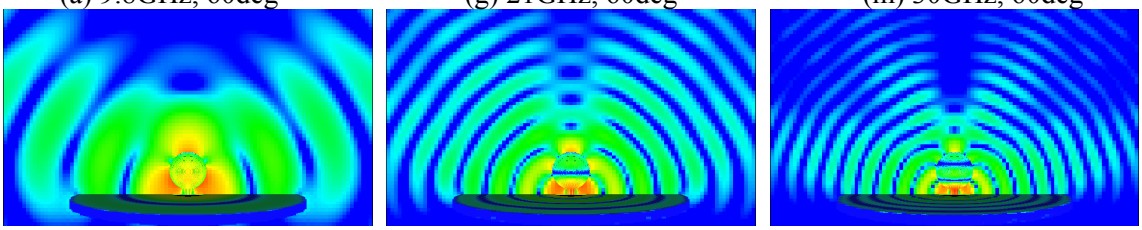

(a) 9.8GHz, 90deg (g) 21GHz, 90deg (m) 30GHz, 90deg

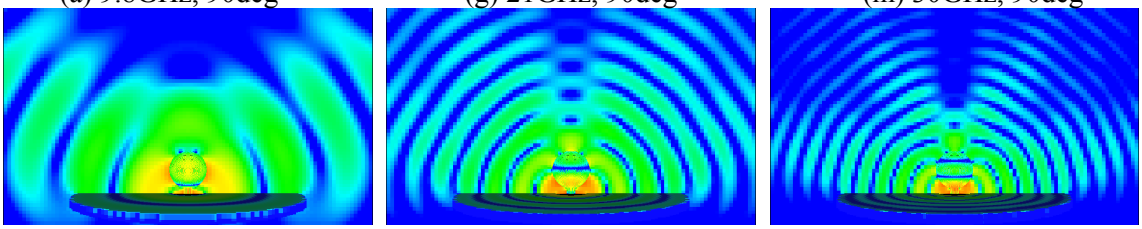

(a) 9.8GHz, 120deg (g) 21GHz, 120deg (m) 30GHz, 120deg

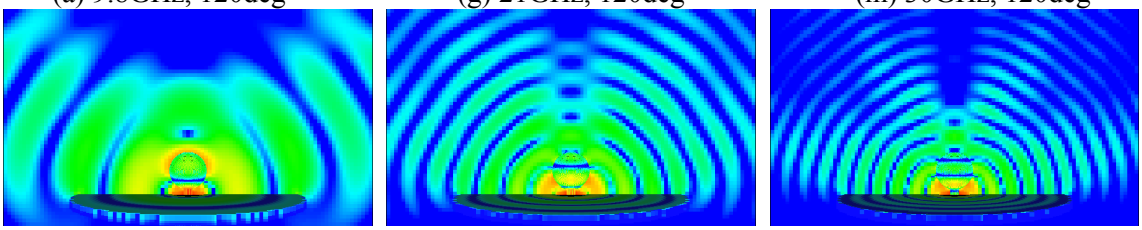

(a) 9.8GHz, 150deg (g) 21GHz, 150deg (m) 30GHz, 150deg

Figure 7: Surface Current and Electric Field